JBC EDITORS' PICK

The palmitoyl acyltransferases ZDHHC5 and ZDHHC8 are uniquely present in DRG axons and control retrograde signaling via the Gp130/JAK/STAT3 pathway

Received for publication, April 11, 2020, and in revised form, September 11, 2020 Published, Papers in Press, September 21, 2020, DOI 10.1074/jbc.RA120.013815

Kaitlin M. Collura[1], Jingwen Niu[1], Shaun S. Sanders[1], Audrey Montersino[1], Sabrina M. Holland[1], and Gareth M. Thomas[1,2,*]

From the [1]Shriners Hospitals Pediatric Research Center (Center for Neurorehabilitation and Neural Repair) and the [2]Department of Anatomy and Cell Biology, Lewis Katz School of Medicine at Temple University, Philadelphia, Pennsylvania, USA

Edited by Roger J. Colbran

Palmitoylation, the modification of proteins with the lipid palmitate, is a key regulator of protein targeting and trafficking. However, knowledge of the roles of specific palmitoyl acyltransferases (PATs), which catalyze palmitoylation, is incomplete. For example, little is known about which PATs are present in neuronal axons, although long-distance trafficking of palmitoyl-proteins is important for axon integrity and for axon-to-soma retrograde signaling, a process critical for axon development and for responses to injury. Identifying axonally targeted PATs might thus provide insights into multiple aspects of axonal biology. We therefore comprehensively determined the subcellular distribution of mammalian PATs in dorsal root ganglion (DRG) neurons and, strikingly, found that only two PATs, ZDHHC5 and ZDHHC8, were enriched in DRG axons. Signals via the Gp130/JAK/STAT3 and DLK/JNK pathways are important for axonal injury responses, and we found that ZDHHC5 and ZDHHC8 were required for Gp130/JAK/STAT3, but not DLK/JNK, axon-to-soma signaling. ZDHHC5 and ZDHHC8 robustly palmitoylated Gp130 in cotransfected nonneuronal cells, supporting the possibility that Gp130 is a direct ZDHHC5/8 substrate. In DRG neurons, *Zdhhc5/8* shRNA knockdown reduced Gp130 palmitoylation and even more markedly reduced Gp130 surface expression, potentially explaining the importance of these PATs for Gp130-dependent signaling. Together, these findings provide new insights into the subcellular distribution and roles of specific PATs and reveal a novel mechanism by which palmitoylation controls axonal retrograde signaling.

The protein-lipid modification palmitoylation is important for the regulation of protein targeting and trafficking in all eukaryotic cells (1, 2). Palmitoylation might be expected to be particularly important in neurons, whose complex morphology and high degree of cellular polarity requires precise trafficking of proteins to specific subcellular locations (2, 3). Consistent with this notion, genetic mutations or targeted mouse knockouts of several members of the ZDHHC (zinc finger DHHC domain–containing) family of palmitoyl acyltransferases (PATs, which catalyze palmitoylation) result in predominantly neuropathological phenotypes (2, 4).

Significant recent progress has been made regarding neuronal roles and substrates of specific PATs (2, 4). However, research has largely focused on roles of PATs in central neurons and in particular how PATs regulate post-synaptic targeting and trafficking of neurotransmitter receptors and their associated scaffold and structural proteins (*e.g.* see Refs. 2 and 5–13). In contrast, far less is known regarding two key aspects of palmitoylation-dependent neuronal regulation. First, PAT expression and subcellular localization in neurons of the peripheral nervous system (PNS) remain to be determined. Second, although key regulators of axon growth, axon guidance, axon maintenance, and presynaptic neurotransmitter release are palmitoylated (*e.g.* see Refs. 2 and 14–19), far less is known regarding the roles and substrates of specific PATs in axons.

One process that is particularly important in peripheral axons is axon-to-soma retrograde signaling, in which proteins are physically transported from distal sites to activate transcription (20, 21). Axonal retrograde signaling plays key roles during neurodevelopment, when both pro-death and pro-survival signals are retrogradely conveyed along axons that are competing for limiting amounts of target-derived neurotrophic factors (22–25). Retrograde signaling in peripheral axons is also critical to activate pro-regenerative transcription post-injury in multiple models (20, 21, 26, 27). We recently reported that one important retrograde signaling protein, dual leucine-zipper kinase (DLK), is palmitoylated and that this modification is essential for DLK-dependent responses to axonal injury in dorsal root ganglion (DRG) sensory neurons (28). Interestingly, other retrograde signaling proteins have been identified in high throughput palmitoyl-proteomic studies from several different cell types (29–33). Prominent among these potentially palmitoylated proteins is Gp130 (gene name *IL6ST*), an obligate component of receptor signaling complexes for the neuropoietic cytokines interleukin-6 (IL-6), ciliary neurotrophic factor (CNTF), leukemia inhibitory factor (LIF), cardiotrophin-1 (CT-1), and oncostatin-M (OSM) (34). Gp130-containing receptor complexes respond to these neuropoietic cytokines by triggering activation of Janus kinases (JAKs), which in turn phosphorylate and activate signal transducer and activator of transcription-3 (STAT3) signaling. Gp130/JAK/STAT3 signals are heavily implicated in axonal retrograde signaling (20, 35–37), and Gp130 is highly expressed in DRG neurons in culture and *in vivo* (38–40). However, whether Gp130 is endogenously palmitoylated in DRG neurons has

This article contains supporting information.

* For correspondence: Gareth Thomas, gareth.thomas@temple.edu.

not been reported, and whether a specific PAT(s) is important for Gp130/JAK/STAT3 signaling is unknown.

Here, we determined the distribution of mammalian PATs in axons of mammalian DRG sensory neurons, a cell type that has provided key insights into neurodevelopment and mechanisms of neurodegeneration (23–25, 38). Only two of the 23 PATs, the closely related ZDHHC5 and ZDHHC8, were enriched in DRG axons. We assessed the functional importance of ZDHHC5/8 and found that these PATs are required for Gp130-dependent, but not DLK-dependent, axonal retrograde signaling. Consistent with this requirement, we found that Gp130 is indeed highly palmitoylated and is an excellent ZDHHC5/8 substrate in transfected cells. In DRG neurons, *Zdhhc5/8* knockdown reduced Gp130 palmitoylation and even more markedly reduced surface levels of Gp130, plausibly explaining why these two PATs are critical for Gp130-dependent signaling. Together, these findings identify the first axonally enriched PATs and provide new insights into the control of axonal retrograde signaling.

Results

The distribution of PAT enzymes in PNS neurons is essentially unknown. We therefore first sought to comprehensively determine the distribution of mammalian PATs in primary cultured DRG neurons, a widely used PNS cell type that is highly relevant for studies of neurodevelopment and nerve injury (38, 41, 42). Previous RNA-Seq data suggest that DRG neurons express mRNAs for all 23 mammalian PATs (38, 39). In parallel work, we have found that one of these PATs, ZDHHC17, is restricted to the soma of DRG neurons (43). However, we were particularly interested in whether specific PATs might localize to DRG axons. We therefore expressed N-terminally HA-tagged forms of the remaining ZDHHC-PATs in primary DRG neurons, using lentiviral delivery to keep levels of exogenously expressed PATs low and thus minimize potential artifacts due to overexpression. All HA-tagged PATs were detected immunocytochemically when virally infected (Fig. 1*A*). Strikingly, we found that axonal enrichment of two PATs, ZDHHC5 and its close homolog ZDHHC8 (2), was significantly greater than that of all other PATs examined (Fig. 1, *A* and *B*).

In contrast to ZDHHC5 and ZDHHC8, all other PATs were detected at higher levels in DRG neuronal cell bodies than in axons, when compared with a freely soluble marker, GFP (Fig. 1, *A* and *B*). Of these somatically enriched PATs, several (ZDHHC3, ZDHHC7, ZDHHC9, ZDHHC11, ZDHHC12, ZDHHC13, ZDHHC14, ZDHHC15, ZDHHC16, ZDHHC21, and ZDHHC23) displayed a discrete perinuclear appearance that overlapped with the Golgi marker GM130 (Fig. S1). Line-scan analysis confirmed co-localization of each of these PATs with GM130, further supporting the hypothesis that this subset of PATs is Golgi-localized (Fig. S1). Several of the remaining PATs that were not enriched in axons (ZDHHC2, ZDHHC4, ZDHHC6, ZDHHC18, ZDHHC19, and ZDHHC25; Fig. 1*A*) displayed a more reticular appearance in DRG neuronal cell bodies. Two of these PATs (ZDHHC4 and ZDHHC6) are reported to localize to the endoplasmic reticulum (ER) in other cell types (44, 45), suggesting that this reticular pattern represents ER membranes.

In these viral expression experiments, the most heavily enriched axonal PAT was ZDHHC5. Using an antibody whose specificity we had confirmed in other neuron types (7), we therefore assessed the expression and subcellular distribution of endogenous ZDHHC5 in DRG neurons. On Western blots, the ZDHHC5 antibody detected a band of the predicted molecular weight of ZDHHC5 in whole-cell lysates from WT DRG neurons infected with a control lentivirus (Fig. 2*A*). This band was almost completely eliminated in lysates from neurons infected with lentivirus expressing an shRNA that knocks down ZDHHC5 (7), suggesting that the antibody also specifically detects ZDHHC5 in DRG neurons (Fig. 2*A*; quantified in Fig. S2*A*). Western blotting of lysates from DRG neurons cultured in microfluidic chambers, which allow specific biochemical isolation of material from distal axons (28, 46), revealed that endogenous ZDHHC5 was strongly detected in distal axonal fractions. Two proteins known to be present in axons, growth-associated protein-43 (GAP-43) and tubulin, were strongly detected in these distal axonal fractions, but histone H3, a nuclear marker, was not (Fig. 2*B*). When used in immunocytochemical studies, the ZDHHC5 antibody detected a robust signal in DRG axons that was again greatly reduced by *Zdhhc5* shRNA knockdown (Fig. 2*C*; quantified in Fig. S2*B*). Together, these data suggest that endogenous and exogenously expressed forms of ZDHHC5 localize to axons of DRG neurons.

We next used microfluidic cultures of DRG neurons to address potential functional roles for ZDHHC5/8 in axonal retrograde signaling. One major retrograde signaling pathway with an important role in DRG neurons involves the kinase DLK, which triggers phosphorylation of the transcription factor c-Jun, via DLK's "downstream" target c-Jun N-terminal kinase (JNK). DLK is palmitoylated, and we previously reported a requirement for DLK palmitoylation in retrograde signaling following axotomy (28). Distal axotomy markedly increased c-Jun phosphorylation in DRG neuron cell bodies in microfluidic cultures infected with a control (GFP-expressing) lentivirus (Fig. 3*A*), consistent with prior results (28). However, axotomy-induced c-Jun phosphorylation was not significantly reduced in *Zdhhc5/*8 "knockdown" microfluidic cultures (Fig. 3, *A* and *B*). These results suggest that axotomy-induced retrograde signaling by the DLK/JNK pathway is ZDHHC5/8-independent.

A second retrograde signaling pathway in DRG neurons can be activated by CNTF and related neuropoietic cytokines. CNTF binds a receptor complex involving Gp130 (gene name *Il6st*), leading to activation of JAK family kinases and phosphorylation of STAT family transcription factors (47–50). Gp130/JAK/STAT3-dependent signaling in DRG neurons has been implicated in neurodevelopment and in responses to nerve injury (51, 52). The addition of CNTF to distal axons of DRG microfluidic cultures infected with control (GFP-expressing) lentivirus markedly increased STAT3 phosphorylation in neuronal cell bodies (Fig. 3*C*). However, in contrast to its lack of effect on axotomy-induced c-Jun phosphorylation, *Zdhhc5/8* knockdown significantly attenuated CNTF-induced STAT3 phosphorylation (Fig. 3, *C* and *D*). These findings suggested that ZDHHC5/8 are required for CNTF-dependent axonal

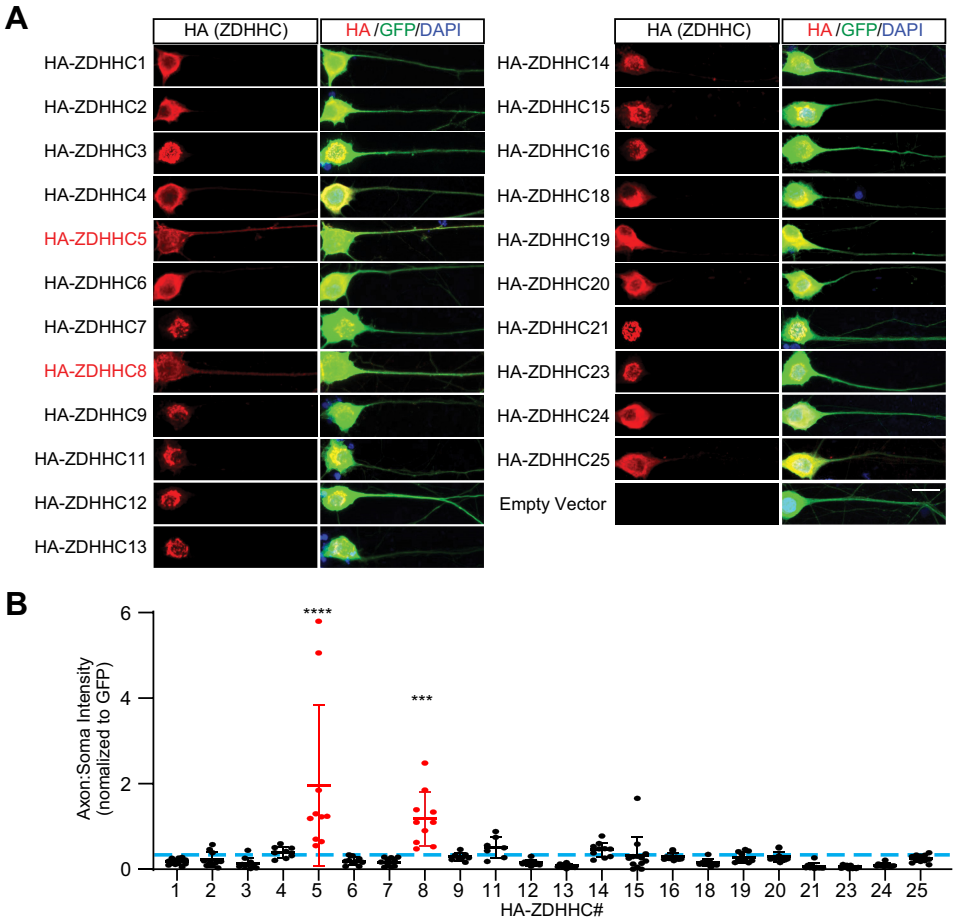

Figure 1. ZDHHC5 and ZDHHC8 are preferentially targeted to DRG axons compared with all other PATs. *A*, images of HA fluorescent signal (*left panels*) and merged HA, GFP, and DAPI (*blue*, to detect nuclei) signals (*right panels*) from individual cultured DRG neurons co-infected with control lentivirus expressing GFP plus a second virus expressing the indicated HA-tagged ZDHHC-PAT. PAT numbering reflects updated gene names (2). *Scale bar*, 20 μm. *B*, quantified axon/soma fluorescence intensity ratio for each of the indicated PATs, normalized to GFP. *Blue dotted line*, mean axon/soma fluorescence intensity ratio for all PATs from all determinations. One-way ANOVA was used with the Bonferroni post hoc test ($F(23, 220) = 9.332$, $p < 0.0001$); ****, $p < 0.0001$; **, $p < 0.01$, compared with average axon/soma ratio for all PATs from all determinations. $n = 7$–13 neurons/condition. *Bars*, mean ± S.D. (*error bars*).

retrograde signaling. Western blotting of parallel conventionally cultured DRG neurons confirmed that the shRNAs used in our microfluidic culture experiments effectively reduced endogenous ZDHHC5 and ZDHHC8 protein levels (Fig. 3*E* and Fig. S2 (*A* and *C*)).

We next sought to identify proteins in the CNTF/Gp130/JAK/STAT3 pathway whose palmitoylation and/or subcellular localization might be regulated in a ZDHHC5/8-dependent manner. Gp130 itself has been identified as a potential palmitoyl-protein in several proteomic studies from nonneuronal cells (29–31, 33) and is highly expressed in DRG neurons (38–40). In addition, ZDHHC5 and ZDHHC8 have both been identified as cell surface-localized PATs (13, 53–55), and Gp130 must also localize to the cell surface to control responses to extracellular neuropoietic cytokines (34, 36, 56). We therefore first used acyl biotinyl exchange (ABE) (7, 57), a nonradioactive palmitoylation assay, to determine whether Gp130 is indeed palmitoylated. We observed a robust signal for palmitoyl-Gp130 in ABE fractions from transfected HEK293T cells (Fig. 4*A*). Gp130 signal was not detected in ABE fractions generated in the absence of the key reagent hydroxylamine and was not detected in ABE fractions from cells that had been treated with the broad-spectrum palmitoylation inhibitor 2-bromopalmitate (*2BP*) (58) (Fig. 4*A*). Together, these findings suggest that Gp130 is indeed palmitoylated.

To address whether Gp130 is a direct substrate for ZDHHC5 and/or ZDHHC8 we co-expressed Gp130 in HEK293T cells with each of these PATs individually. Gp130 palmitoylation was significantly increased by WT forms of both ZDHHC5 and ZDHHC8 but not by their respective transferase-dead mutants (ZDHHS5 and ZDHHS8) (Fig. 4, *B*–*E*). These findings suggest that both ZDHHC5 and ZDHHC8 can directly palmitoylate Gp130.

We next examined whether Gp130 is endogenously palmitoylated in DRG neurons. We observed a robust Gp130 signal in ABE fractions from cultured DRG neuronal lysates, suggesting that Gp130 is endogenously palmitoylated in DRG neurons (Fig. 4*F*). Gp130 palmitoylation was significantly reduced in *Zdhhc5/8* knockdown neurons (Fig. 4, *F* and *G*). However, we also observed a trend toward reduced Gp130 total expression levels in *Zdhhc5/8* knockdown neurons (Fig. 4*H*). This latter effect did not reach statistical significance but likely accounted for the fact that Gp130 palmitoylation was not significantly reduced by *Zdhhc5/8* knockdown when normalized to total

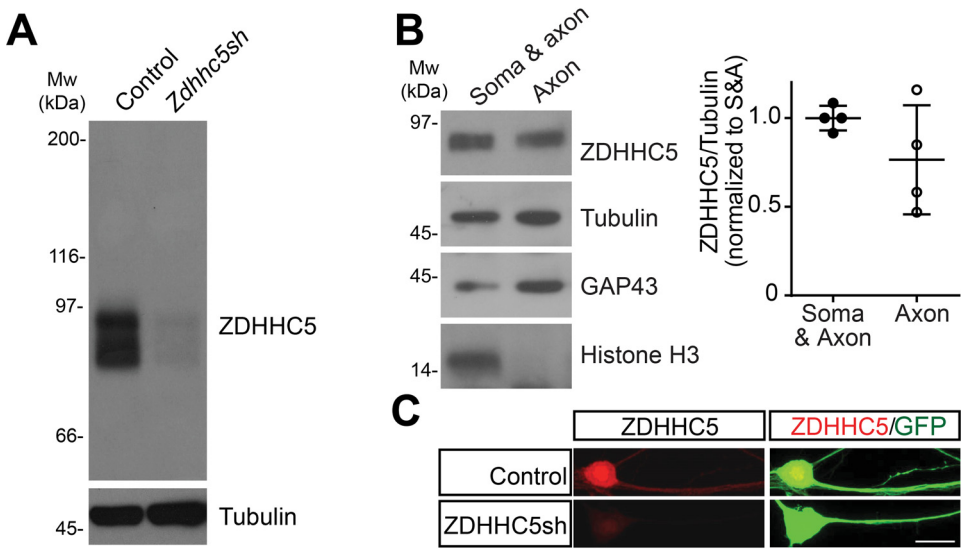

Figure 2. Endogenous ZDHHC5 localizes to axons in DRG neurons. *A*, cultured DRG neurons were infected with either control virus or virus expressing shRNA against ZDHHC5 (*ZDHHC5sh*). *Zdhhc5* knockdown was verified by immunoblotting lysates of infected neurons. Molecular weight markers (*Mw (kDA)*) are indicated on the *left-hand side* of this and all subsequent blots. The efficacy of ZDHHC5 knockdown in this and replicate experiments is quantified in Fig. S2. *B*, DRG neurons were cultured in microfluidic chambers and proximal chambers (containing cell somas and proximal axons (*Soma & axon*)) and distal chambers (containing distal axons but no neuronal cell bodies (*Axon*)) were lysed separately in denaturing buffer. Equivalent volumes of each fraction were subjected to SDS-PAGE and immunoblotted with the indicated antibodies. Endogenous ZDHHC5 is clearly detected in distal axon fractions. *Right panel plot*, quantified ZDHHC5 in the indicated microfluidic compartments, relative to tubulin ($n = 4$ determinations). *C*, images of DRG neurons infected with lentivirus expressing GFP with or without *Zdhhc5* shRNA, following fixation and immunostaining with the indicated antibodies. *Zddhc5* knockdown greatly reduces axonal signal recognized by the anti-ZDHHC5 antibody (quantified in Fig. S2). *Scale bar*, 20 μm. *Bars*, mean ± S.D. (*error bars*).

Gp130 levels (Fig. 4*I*). Neither palmitoyl nor total levels of another axonal palmitoyl-protein, GAP-43, were affected by *Zdhhc5/8* knockdown (Fig. 4*F*), consistent with a report that GAP-43 is likely palmitoylated by different ZDHHC-PATs (59).

We then asked whether ZDHHC5/8 might exert additional effects on Gp130 in DRG neurons. In particular, we performed surface biotinylation assays to address whether ZDHHC5/8 are required for stable targeting of Gp130 to the neuronal cell surface. *Zdhhc5/8* knockdown markedly reduced Gp130 levels in surface fractions of DRG neurons (Fig. 5, *A* and *B*). Surface levels of another axonal transmembrane palmitoyl-protein, neurofascin, were not significantly affected by *Zdhhc5/8* knockdown, suggesting that ZDHHC5/8 loss does not indiscriminately affect surface expression of axonal palmitoyl-proteins (Fig. 5, *A* and *B*). The intracellular protein ERK was not detected in surface fractions, confirming the fidelity of these preparations (Fig. 5*A*). These findings suggest that ZDHHC5/8 are critical for normal cell surface localization of Gp130, a requirement consistent with the importance of these PATs for Gp130-dependent retrograde signaling.

Discussion

Genetic studies suggest that specific PATs play particularly important roles in the nervous system (60–62), but most research has focused on identifying synaptodendritic PAT substrates. In contrast, far less has been reported regarding the roles of specific PATs, and of palmitoylation in general, in axons. Our comprehensive assessment of PAT subcellular targeting in primary DRG neurons reveals that the related PATs ZDHHC5 and ZDHHC8 are specifically enriched in DRG axons, compared with other PATs. Moreover, ZDHHC5/8 play key roles in the localization and signaling of the axonal retrograde signaling protein Gp130.

Our assessment of PAT localization in DRG neurons invites comparisons with reports of PAT distribution in other cell types. Interestingly, our finding that ZDHHC5 and ZDHHC8 are the PATs that most readily escape the confines of the ER/Golgi in DRG neurons (Fig. 1) is consistent with reports from two other polarized cell types, hippocampal neurons and Madin–Darby canine kidney epithelial cells. In both of these cell types, many PATs are restricted to the ER/Golgi, but ZDHHC5 and ZDHHC8 are not (7, 13, 55, 63). Interestingly, however, other PATs, such as ZDHHC1, ZDHHC2, and ZDHHC11, remain confined to the somatic ER/Golgi in DRG neurons, but not in hippocampal neurons (12, 64, 65). This differential targeting could potentially be explained if pseudounipolar DRG neurons, whose peripheral and central projections both morphologically resemble axons, lack certain elements of the targeting machinery used by hippocampal neurons to transport these PATs to dendrites.

Although our findings are broadly consistent with other work from polarized nonneuronal cells (55), it is nonetheless perhaps surprising that all PATs except ZDHHC5 and ZDHHC8 were relatively confined to the DRG neuronal soma, compared with axons. However, it is important to appreciate that small amounts of these PATs, below the threshold for detection in our experiments, may still play key functional roles in axons. Moreover, enrichment of specific PATs in DRG axons may be greater at different developmental stages and/or under different conditions. In particular, we recognize that our study was performed using embryonic DRG neurons and that PAT distribution may differ in mature and/or aged DRG neurons. On a similar note, expression of the PAT ZDHHC23 increases

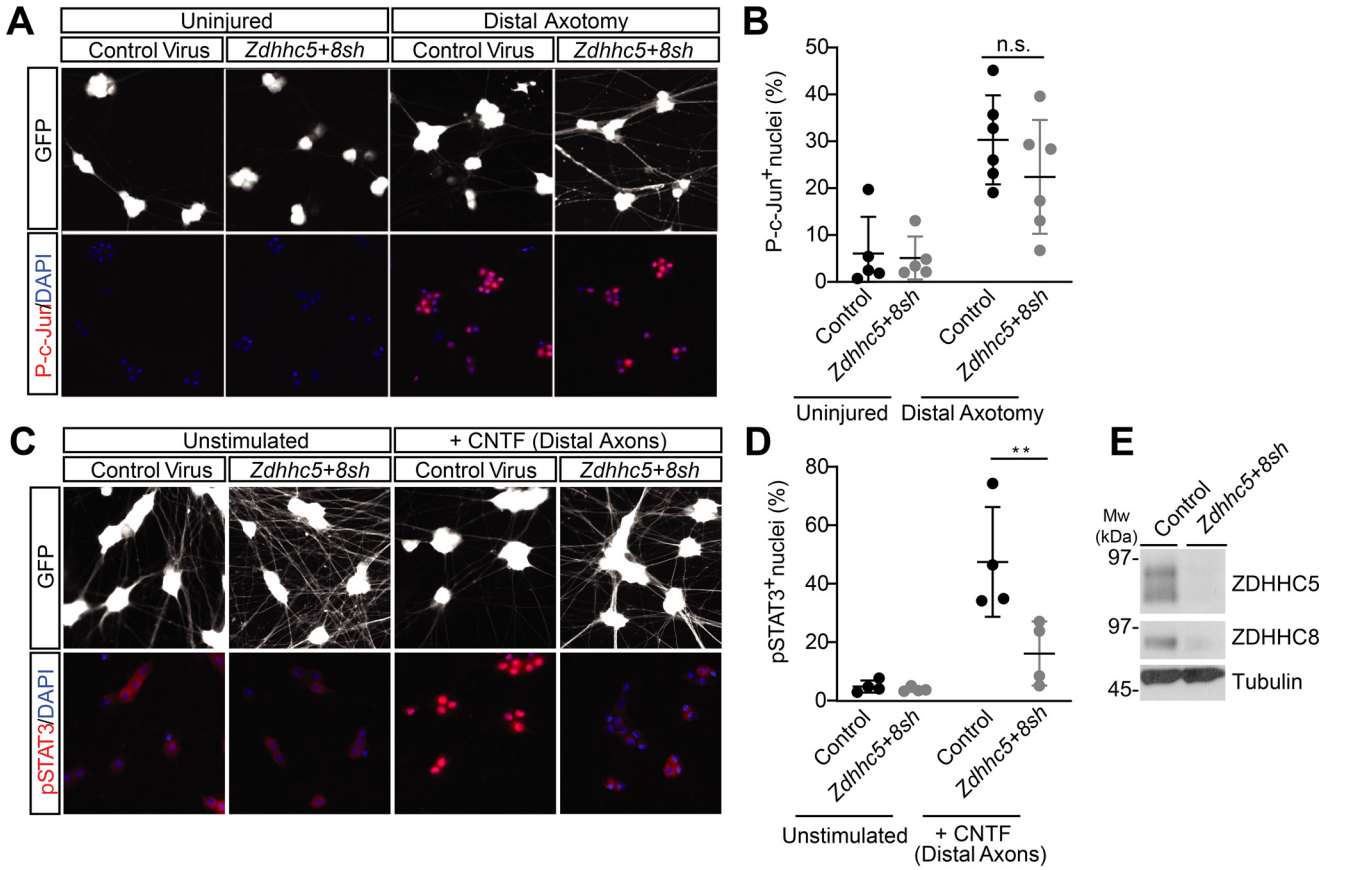

Figure 3. ZDHHC5/8 are critical for retrograde signaling by the Gp130/JAK/STAT3 pathway, but not the DLK/JNK pathway. *A*, DRG neurons cultured in microfluidic chambers were infected with the indicated viruses. Cultures were left untreated, or distal axons were axotomized by aspiration. Cell body chambers were then immunostained to detect phospho-c-Jun (*p-c-Jun*) and DAPI. *B*, quantified data from *A* reveal that axotomy-induced c-Jun phosphorylation, which is strongly DLK-dependent (28), is not affected by *Zdhhc5/8* knockdown. *ns*, not significantly different from control-infected axotomized condition, two-way ANOVA: virus $p = 0.2754$ ($F(1, 18) = 1.265$), axotomy $p < 0.0001$ ($F(1, 18 = 27.89$), interaction $p = 0.3892$ ($F(1, 18) = 0.7785$), $n = 5$–6 determinations/condition. *C*, distal axonal chambers of DRG neurons cultured as in *A* were treated with or without 10 ng/ml rat CNTF, and cell body chambers were fixed and immunostained to detect STAT3 phosphorylation (pSTAT3) and DAPI. *D*, quantified data from *C* reveal that *Zdhhc5/8* knockdown significantly reduces axotomy-induced STAT3 phosphorylation. $n = 4$ determinations/condition. **, $p < 0.01$, two-way ANOVA: virus $p = 0.0119$ ($F(1, 12) = 8.766$), treatment $p = 0.0003$ (F (1, 12) = 25.27), interaction $p = 0.0166$ ($F(1, 12) = 7.74$). *E*, Western blots of lysates from conventionally cultured DRG neurons (sister cultures of those used for microfluidic experiments in *A–D*) infected with the indicated viruses confirm effective reduction of ZDHHC5 and ZDHHC8 protein levels by their respective shRNAs (see also quantified data in Fig. S2). *Bars*, mean ± S.D. (*error bars*).

>6-fold in DRGs after transection of the sciatic nerve, a major nerve via which DRG axons project into peripheral tissues (66). This finding raises the possibility that ZDHHC23, and potentially other PATs, plays different roles and/or operates in different subcellular locations in healthy and injured DRG neurons. This is an interesting area of investigation for future work. Last, whereas both immunocytochemical and biochemical analyses suggest that virally expressed and endogenous ZDHHC5 are both targeted to DRG axons (Figs. 1 and 2), we recognize that localization of other virally expressed PATs might not fully phenocopy that of their endogenous counterparts.

A related question is whether ZDHHC5 or ZDHHC8 dominantly controls Gp130 palmitoylation and/or localization. In preliminary experiments, we found that *Zdhhc8* knockdown more markedly reduced Gp130 surface localization than did *Zdhhc5* knockdown.[3] However, in general, we found that combined *Zdhhc5/8* knockdown was required to more effectively reduce Gp130 palmitoylation and therefore focused on effects caused by the combined loss of these PATs.

The likely localization of ZDHHC5 and ZDHHC8 to the axonal plasma membrane provides a plausible explanation for why loss of these PATs markedly decreases Gp130 surface expression (Fig. 5*A*). However, we note that loss of ZDHHC5/8 only partially reduces Gp130 palmitoylation (Fig. 4*F*), raising the possibility that other PATs may palmitoylate Gp130 in other cellular locations prior to its delivery to the plasma membrane. Another key factor to consider is that detection of Gp130 by ABE does not distinguish between different sites of Gp130 palmitoylation. It is hence possible that ZDHHC5/8 palmitoylate Gp130 at a site(s) that is more important for surface expression and/or signaling, whereas other sites on Gp130 are palmitoylated by different PATs. Another important point is that *Zdhhc5/8* knockdown reduces Gp130 palmitoylation but also causes an apparent (although not statistically significant) reduction in Gp130 total expression (Fig. 4, *F–I*). We and others have reported that *Zdhhc5/8* knockdown reduces palmitoylation of ZDHHC5/8 substrates in other neuronal types, without

[3] K. M. Collura and G. M. Thomas, unpublished observations.

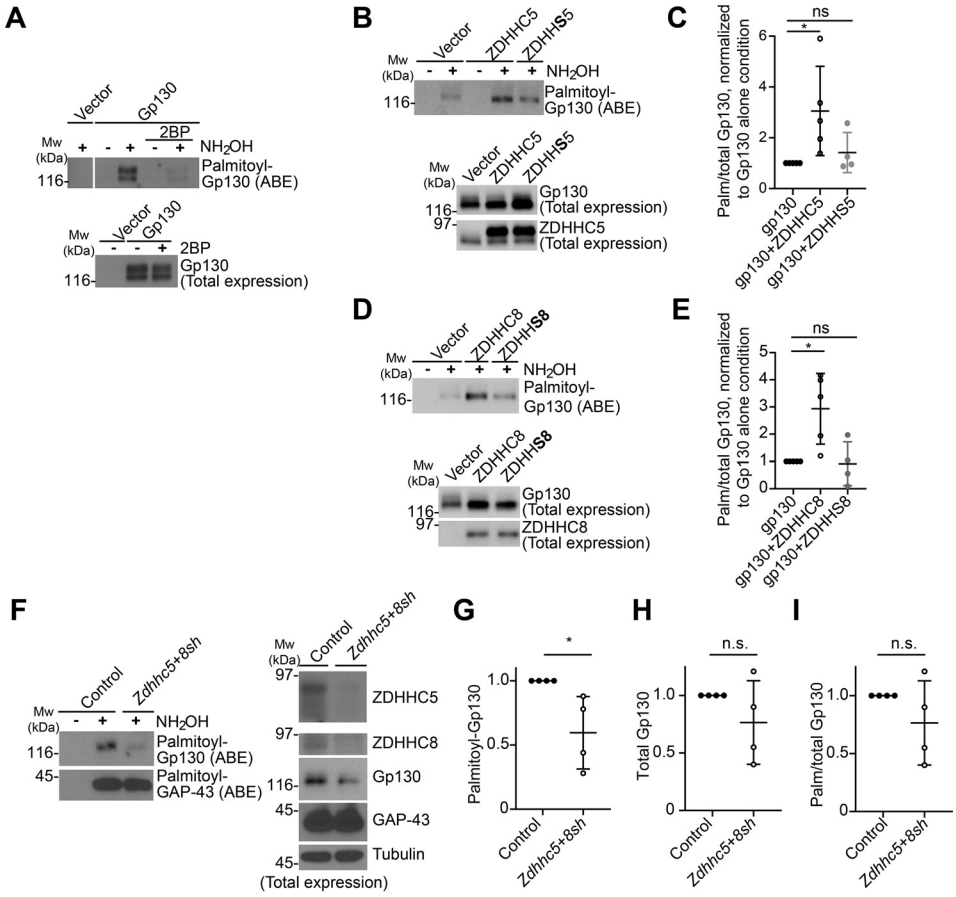

Figure 4. Gp130 is palmitoylated in a ZDHHC5/8-dependent manner. *A*, HEK293T cells were transfected with an empty vector or with Gp130-expressing vector and subsequently treated with palmitoylation inhibitor 2-bromopalmitate (*2BP*) or vehicle. ABE fractions were prepared and blotted to detect palmitoyl-Gp130 (*top*). Lysates were blotted to detect total Gp130 expression (*bottom*). The image in the *top panel* is from a single Western blot analysis, cropped to remove intervening spacer lanes. The experiment shown is representative of three individual determinations. *B*, HEK293T cells were transfected with Gp130 cDNA plus the indicated ZDHHC5 or ZDHHS5 cDNAs and ABE assays performed. ABE fractions were blotted to detect palmitoyl-Gp130 (*top*). Lysates were blotted to detect total Gp130 and total ZDHHC5 expression (*middle* and *bottom panels*). *C*, quantified data for palmitoylated-to-total (*Palm/total*) Gp130 from *B* confirm that ZDHHC5 significantly increases Gp130 palmitoylation, whereas catalytically inactive ZDHHS5 does not. *, $p < 0.05$, nonparametric one-way ANOVA with Dunn's multiple-comparison post hoc test ($p = 0.0086$, Kruskal–Wallis statistic = 7.848), 4–5 determinations/condition. *D*, as in *B*, except that cells were transfected with the indicated ZDHHC8 or ZDHHS8 cDNAs, and lysates were blotted with Gp130 and ZDHHC8 antibodies. *E*, quantified data from *D* confirm that ZDHHC8 significantly increases palmitoyl-Gp130 levels, whereas catalytically inactive ZDHHS8 does not. *, $p < 0.05$, nonparametric one-way ANOVA with Dunn's multiple-comparison post hoc test ($p = 0.0086$, Kruskal–Wallis statistic = 7.848), 4–5 determinations per condition. *F*, cultured sensory neurons were infected with control virus or with viruses expressing ZDHHC5 and ZDHHC8 shRNAs. ABE fractions were prepared from lysates and blotted to detect palmitoyl-Gp130 and -GAP-43 (*left panels*). Lysates were blotted to detect total ZDHHC5, ZDHHC8, Gp130, GAP-43, and tubulin expression (*right panels*). *G*, quantified data from $n = 4$ determinations from *F* confirm that *Zdhhc5/8* knockdown significantly reduces Gp130 palmitoylation. *, $p < 0.05$, *t* test. *H*, quantified data from $n = 4$ determinations from *F* confirm that *Zdhhc5/8* knockdown does not significantly reduce Gp130 total levels. *n.s.*, not significant, *t* test. *I*, quantified data from $n = 4$ determinations from *F* confirm that *Zdhhc5/8* knockdown does not significantly reduce Gp130 palmitoylation, when normalized to total Gp130. *n.s.*, not significant, *t* test. *Bars*, mean ± S.D. (*error bars*).

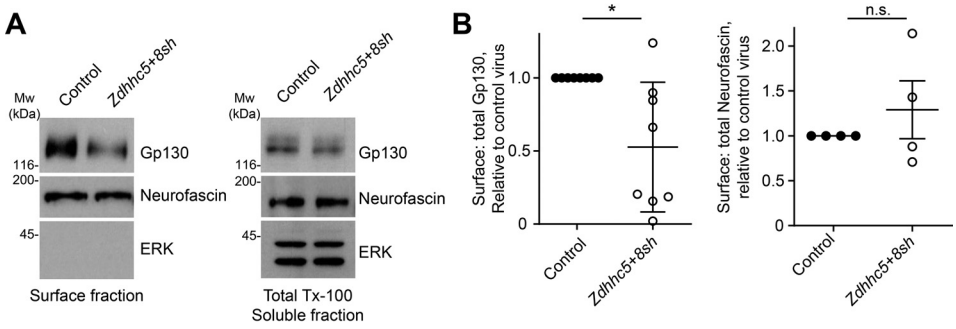

Figure 5. ZDHHC5/8 control Gp130 surface expression. *A*, surface fractions (*left column*) and total lysates from cultured DRG neurons infected with the indicated viruses were immunoblotted with the indicated antibodies. *B*, quantified data from *A* reveal that *Zdhhc5/8* knockdown significantly reduces surface/total Gp130 (*left histogram*; *, $p < 0.05$, *t* test) but does not affect surface/total levels of the axonal palmitoyl-protein neurofascin (*right histogram*; *n.s.*, nonsignificant, *t* test, $n = 8$ and $n = 4$ determinations/condition, respectively). *Bars*, mean ± S.D. (*error bars*).

affecting total expression of those substrates (7, 10). Effects of ZDHHC5/8 loss on protein palmitoylation and total expression can thus sometimes be dissociated. However, analysis of hypomorphic *Zdhhc5* gene trap mice revealed a large number of proteins whose palmitoyl and total levels were similarly reduced in the absence of ZDHHC5 (67). It therefore appears that palmitoylation is closely coupled to protein stability for several ZDHHC5 substrates, potentially including Gp130.

Our study did not directly address the physical effect of palmitoylation on Gp130 localization and/or trafficking at the molecular level. However, one intriguing possibility is that palmitoylation targets Gp130 to lipid rafts, detergent-insoluble regions of the cell membrane to which palmitoyl-proteins often localize (68). Consistent with this possibility, several studies have detected Gp130 in lipid rafts (69–74). Importantly, whereas Gp130 localization to lipid rafts appears to be constitutive in nonneuronal cells (69–71), a portion of Gp130 rapidly translocates to lipid rafts in a neuroblastoma cell line after CNTF treatment (71). Although the importance of Gp130 raft localization for downstream signaling may differ depending on the cell type or stimulus (71–74), lipid raft localization is thus one possible consequence of Gp130 palmitoylation. However, palmitoylation could equally plausibly control other aspects of Gp130 trafficking. Perhaps most notably, palmitoylation by ZDHHC5 controls local trafficking of the ZDHHC5 substrate δ-catenin into dendritic spines in hippocampal neurons (10, 13). It is thus possible that palmitoylation promotes trafficking of Gp130 to the surface of axons from intracellular locations. Such a role would not be mutually exclusive with the raft localization described above. Further studies, perhaps combining biochemical fractionation approaches with live imaging experiments, could provide more insights into this issue.

We also recognize that the effect of *Zdhhc5/8* knockdown on Gp130 surface expression may involve additional substrate(s) regulated by these PATs. However, several findings support the hypothesis that this effect is due to direct palmitoylation of Gp130. First, Gp130 is the only member of this membrane receptor complex that is known to be palmitoylated, a modification reported in four proteomic studies and confirmed by our own targeted experiments. In contrast, the direct receptor for CNTF (CNTF-R) is unlikely to be palmitoylated as it is a glycosylphosphatidylinositol-linked extracellular protein (75). Moreover, the LIF receptor (LIFR) (which forms part of many Gp130 signaling complexes) has never been identified as a palmitoyl-protein in nearly 40 studies (3, 76). These findings suggest that Gp130 itself is likely the only element of the Gp130/CNTF-R/LIFR complex that is directly palmitoylated by ZDHHC5/8, increasing the likelihood that effects of *Zdhhc5/8* knockdown on Gp130 surface localization are direct.

The importance of direct palmitoylation for Gp130 plasma membrane localization and/or signaling could be more directly assessed using a nonpalmitoylated shRNA-resistant Gp130 cysteine mutant after knockdown of endogenous Gp130 (*Il6st*). However, Gp130 contains several intracellular cysteines, and we have yet to map specific sites of Gp130 palmitoylation in neurons. This issue complicates the assessment of plasma membrane localization and signaling of nonpalmitoylated Gp130, although we nonetheless appreciate the importance of assessing the extent to which direct Gp130 cysteine mutations phenocopy effects of *Zdhhc5/8* knockdown.

Even if ZDHHC5/8 directly control Gp130 targeting, we cannot exclude the possibility that effects of *Zdhhc5/8* knockdown on CNTF-induced Gp130/JAK/STAT3 signaling involve additional palmitoyl-protein(s). Importantly, however, *Zdhhc5/8* knockdown did not affect axotomy-induced retrograde signaling via the parallel DLK/JNK/c-Jun pathway (Fig. 3, *A* and *B*). These findings increase the likelihood that the reduced palmitoylation and surface expression of Gp130 in *Zdhhc5/8* knockdown neurons directly accounts for attenuated Gp130/JAK/STAT3 signaling.

Finally, combining the findings from this study with prior results from our own group and others reveals that palmitoylation is an important modification that controls both anterograde and retrograde signaling in axons (*e.g.* see Refs. 18, 19, 28, and 77). It will be of great interest to gain further understanding of the regulation of palmitoylation in these contexts and to determine whether palmitoylation is similarly important for other axonal transport pathways in physiological and/or pathological settings (78–81).

Experimental procedures

Antibodies

The following antibodies, from the indicated sources, were used: anti-ZDHHC5 (rabbit) (Sigma Prestige); anti-HA11 (16B12, mouse) (Covance); anti-GFP (clone 3E6, mouse) (Life Technologies); anti-ZDHHC8 (rabbit) (Santa Cruz Biotechnology, Inc.); anti-GM130 (rabbit) (Abcam); anti-Gap43 (rabbit) (Novus Biologicals); anti-pan-neurofascin (mouse) (NeuroMab); and anti-phospho-c-Jun (Ser-63, rabbit), anti-ERK1/2 (mouse), anti-GP130 (rabbit), and anti-phospho-STAT3 (Tyr-705, rabbit) (all from Cell Signaling Technologies).

Molecular biology

Human GP130 (gene name *IL6ST*) cDNA (DNASU) was amplified by PCR and inserted into an untagged modified lentiviral vector FEW (28). cDNAs coding for the mouse ZDHHC proteins 1, 2, 4–7, 9–16, 19, and 21–23 were a generous gift from Dr. M. Fukata (National Institute of Physiological Sciences, Okazaki, Japan). These *Zdhhc*-PAT cDNAs were then subcloned into the FEW vector in frame with an N-terminal HA tag (FEW-HA-*Zdhhc*). Murine *Zdhhc8*, *18*, and *20* were gene-synthesized (Genewiz) and subcloned into the N-terminally HA-tagged FEW vector. The FEW-HA-*Zdhhc3* plasmid induced toxicity when expressed for the prolonged times needed for lentiviral production in HEK293T cells. Therefore, murine *Zdhhc3* cDNA was subcloned into a further modified N-terminally HA-tagged vector, in which the EF1α promoter was replaced with the synapsin I promoter (FSW-HA-*Zdhhc3*), to ensure neuron-specific expression and prevent HEK293T cell death during lentivirus production. Human *ZDHHC8* cDNA was used in a Myc-His–tagged mammalian expression vector for HEK293T cell experiments (54). Catalytically inactive (DHHC → DHH<u>S</u>) mutants of *Zdhhc5* and *ZDHHC8* were described previously (7).

To knock down *Zdhhc5* expression in DRG neurons, a previously described shRNA (5′-CCTCAGATGATTCCAAGAGAT-3′) (7) was used. To knock down *Zdhhc8* expression, the shRNA (5′-CAGGATGCCACTCTCAGTGAGCCTAAAGC-3′) (Origene) was used.

Transfection and lentiviral production

HEK293T cells were transfected using a calcium phosphate–based method as described (7). Vesicular stomatitis virus G–pseudotyped lentivirus was generated as described (7). For *Zdhhc*-PAT–expressing viruses, HEK293T cells were transfected with individual FEW-HA-*Zdhhc* cDNA (or FSW-HA-*Zdhhc3*) along with lentiviral helper plasmids. Supernatant containing virus was harvested at 48 and 72 h post-transfection, concentrated by centrifugation, and resuspended in neurobasal medium. For knockdown studies, titers of control virus and shRNA-expressing viruses were determined by monitoring GFP expression in infected HEK293T cells. DRG neurons were infected on DIV 4–5 with 1×10^6 to 3×10^6 transduction units of virus for 7–9 days prior to immunocytochemical or biochemical analysis.

Neuronal cultures

Primary neurons were cultured from DRG of embryonic day 15–16 rats as described (28). All procedures involving animals were approved by the Institutional Animal Care and Use Committee of Temple University. DRG neuron cultures were plated on 18-mm round glass coverslips (for immunocytochemical studies), 12-well polystyrene plates (for biochemical studies), or 22 × 40-mm rectangular coverslips with microfluidic chambers (for retrograde signaling and immunocytochemical studies). Coverslips and polystyrene plates were coated with poly-L-lysine and laminin (both from Millipore–Sigma) at 4 °C, washed with deionized water, and air-dried prior to plating of neurons.

Microfluidic chambers were designed and used as described previously (28), based on a prior description (82), and cast using Sylgard 184 (Dow Corning) as per the manufacturer's instructions. DRG neurons were plated in one chamber, and their axons were allowed to grow through the microgrooves into the adjacent chamber.

Neurons were plated at a density of 15,000 cells/well for coverslip cultures, 50,000 cells/well for biochemical cultures, and 35,000 cells for each microfluidic device. Neurons were maintained in neurobasal medium supplemented with B27, GlutaGro (Mediatech) and 25 ng/ml NGF (BD Biosciences or Alomone). Fluorodeoxyuridine (5 μM) was added on DIV 0 to prevent growth of nonneuronal cells.

Biochemical assays

ABE assays were performed as described previously (7), based on a previous protocol (57). For surface biotinylation assays, DRG neurons were infected for 7–9 days with either control or shRNA-expressing lentiviruses and then washed three times with recording buffer (25 mM HEPES, pH 7.4, 0.12 mM sodium chloride, 5 mM potassium chloride, 2 mM calcium chloride, 30 mM glucose, 1 mM Mg^{2+}) on ice. Neurons were then incubated with 1 mg/ml amino-reactive (Sulfo-NHS-SS-) biotin (Thermo Scientific) in recording buffer for 20 min on ice. Neurons were then washed three times with recording buffer on ice and subsequently lysed in IPB buffer containing protease and phosphatase inhibitors (7). Lysates were centrifuged to remove insoluble material, and inputs were made from the soluble fraction. Biotinylated proteins in lysates were captured using Neutravidin-conjugated agarose beads (Thermo Scientific). Beads were then washed three times in IPB buffer (supplemented with 0.5 M NaCl) followed by three washes in IPB buffer, to remove unbound proteins. Purified proteins were eluted from beads using SDS sample buffer and subsequently evaluated by immunoblotting. Western blot analyses were performed as described previously (7) using horseradish peroxidase–coupled secondary antibodies and an enhanced chemiluminescence reagent (PerkinElmer Life Sciences).

Retrograde signaling assays in microfluidic cultures

To evaluate c-Jun phosphorylation postinjury, distal axons of microfluidic cultures were axotomized as described (28) and fixed 4 h later. To evaluate STAT3 phosphorylation following CNTF stimulation, medium in distal axonal chambers of microfluidic cultures was removed and replaced with medium supplemented with 10 ng/ml rat CNTF (R & D Systems). 1 h later, neurons were fixed to assess STAT3 phosphorylation by immunostaining.

Immunocytochemistry and microscopy

For DRG neurons cultured on glass coverslips, cells were fixed in 4% paraformaldehyde (w/v), 4% sucrose (w/v) in PBS for 10 min at room temperature. For microfluidic cultures, 4% paraformaldehyde/sucrose was added to both the cell body and axonal chambers for 5 min prior to removal of the polydimethylsiloxane device. Coverslips were then incubated for an additional 5 min in 4% paraformaldehyde/sucrose at room temperature. Following fixation, all coverslips were washed with PBS, permeabilized with 0.25% (w/v) Triton X-100, and blocked in 10% (v/v) normal goat serum in PBS for 1 h at room temperature before staining with the appropriate primary antibodies overnight at 4 °C. Coverslips were then washed with PBS, incubated with a 1:500 dilution of Alexa Fluor–conjugated secondary antibodies, washed again, and mounted on microscope slides using Fluoromount-G (Southern Biotech). The nuclear dye DAPI (300 nM; Cell Signaling Technologies) was added to one of the washes after secondary antibody incubation.

Image acquisition and analysis

Images of phospho-c-Jun and phospho-STAT3 immunofluorescence were acquired using a Nikon 80i microscope (×10, 0.3 numerical aperture objective). Images of ZDHHC PAT distribution were acquired using a Nikon C2 inverted confocal microscope (oil immersion objective, 60×, 1.3 numerical aperture). Maximum-intensity projections were generated from individual Z slices (1.0-μm spacing, 1024 × 1024-pixel resolution) using NIS Elements software. All images were quantitatively analyzed using ImageJ software. To assess axonal targeting of HA-tagged PATs, an isolated neuron was selected based

on GFP signal. This GFP signal was used to trace the area of the cell soma and an area of distal axon (100 μm from the soma) for an isolated neuron. Intensity of GFP and HA signals (average gray values) in each of these regions was then logged to a spreadsheet. The ratio of GFP fluorescence between these two regions was set as "1" and the intensity of each ZDHHC-PAT's distribution was then calculated relative to this value. For plotting of data in Fig. 1, the average axon/soma fluorescence ratio for distribution of all PATs, from all determinations, was also calculated and used for statistical comparisons. To analyze PAT-GM130 colocalization, the ImageJ line profile plot tool was used to determine the intensity of the HA and GM130 fluorescence signals along a line of set length, drawn across the neuronal soma.

Statistical analysis

The number of replicates for each experiment is shown in the respective figure legends. Data were analyzed using a two-tailed Student's *t* test or one- or two-way ANOVA with Tukey or Bonferroni post hoc test where indicated. Results with a p value <0.05 were assigned statistical significance. Where quantified data are not shown, the number of individual replicate experiments is stated.

Data availability

Source data related to this article will be shared upon reasonable request by the corresponding author: gareth.thomas@temple.edu.

Acknowledgments—We thank members of the Thomas Laboratory and Dr. C. Su (University of California, San Diego) for insightful comments on the manuscript, Dr. Masaki Fukata (National Institute of Physiological Sciences, Okazaki, Japan) for generously providing ZDHHC-PAT cDNAs and Dr. C. Benedict for molecular biological assistance.

Author contributions—K. M. C., J. N., and G. M. T. data curation; K. M. C., S. S. S., and G. M. T. formal analysis; K. M. C., J. N., S. S. S., A. M., and G. M. T. investigation; K. M. C., S. S. S., A. M., and S. M. H. methodology; K. M. C. and G. M. T. writing-original draft; J. N. validation; J. N., S. S. S., A. M., S. M. H., and G. M. T. writing-review and editing; S. M. H. and G. M. T. supervision; G. M. T. conceptualization; G. M. T. funding acquisition; G. M. T. project administration.

Funding and additional information—This work was supported by National Institutes of Health Grant R01 NS094402 and Shriners Hospitals for Children Grant 86610 PHI (to G. M. T.). S. S. received a Brody Family Medical Trust Fund Fellowship. The content is solely the responsibility of the authors and does not necessarily represent the official views of the National Institutes of Health.

Conflict of interest—The authors declare that they have no conflicts of interest with the contents of this article.

Abbreviations—The abbreviations used are: ZDHHC, zinc finger DHHC domain–containing; Gp130, glycoprotein of 130 kDa; JAK, Janus kinase; STAT3, signal transducer and activator of transcription-3; PAT, palmitoyl acyltransferase; DRG, dorsal root ganglion; DLK, dual leucine-zipper kinase; JNK, c-Jun N-terminal kinase; PNS, peripheral nervous system; IL-6, interleukin-6; CNTF, ciliary neurotrophic factor; LIF, leukemia inhibitory factor; CT-1, cardiotrophin-1; OSM, oncostatin-M; ER, endoplasmic reticulum; DAPI, 4',6-diamidino-2-phenylindole; GM130, Golgi matrix protein of 130 kDa; ABE, acyl biotinyl exchange; shRNA, short hairpin RNA; DIV, day *in vitro*; HA, hemagglutinin; ANOVA, analysis of variance; ERK, extracellular signal–regulated kinase.

References

1. Chen, B., Sun, Y., Niu, J., Jarugumilli, G. K., and Wu, X. (2018) Protein lipidation in cell signaling and diseases: function, regulation, and therapeutic opportunities. *Cell Chem. Biol.* **25,** 817–831 CrossRef Medline
2. Fukata, Y., and Fukata, M. (2010) Protein palmitoylation in neuronal development and synaptic plasticity. *Nat. Rev. Neurosci.* **11,** 161–175 CrossRef Medline
3. Sanders, S. S., Martin, D. D., Butland, S. L., Lavallée-Adam, M., Calzolari, D., Kay, C., Yates, J. R., 3rd,., and Hayden, M. R. (2015) Curation of the mammalian palmitoylome indicates a pivotal role for palmitoylation in diseases and disorders of the nervous system and cancers. *PLoS Comput. Biol.* **11,** e1004405 CrossRef Medline
4. De, I., and Sadhukhan, S. (2018) Emerging roles of DHHC-mediated protein *S*-palmitoylation in physiological and pathophysiological context. *Eur. J. Cell Biol.* **97,** 319–338 CrossRef Medline
5. Hayashi, T., Rumbaugh, G., and Huganir, R. L. (2005) Differential regulation of AMPA receptor subunit trafficking by palmitoylation of two distinct sites. *Neuron* **47,** 709–723 CrossRef Medline
6. Hayashi, T., Thomas, G. M., and Huganir, R. L. (2009) Dual palmitoylation of NR2 subunits regulates NMDA receptor trafficking. *Neuron* **64,** 213–226 CrossRef Medline
7. Thomas, G. M., Hayashi, T., Chiu, S. L., Chen, C. M., and Huganir, R. L. (2012) Palmitoylation by DHHC5/8 targets GRIP1 to dendritic endosomes to regulate AMPA-R trafficking. *Neuron* **73,** 482–496 CrossRef Medline
8. Thomas, G. M., Hayashi, T., Huganir, R. L., and Linden, D. J. (2013) DHHC8-dependent PICK1 palmitoylation is required for induction of cerebellar long-term synaptic depression. *J. Neurosci.* **33,** 15401–15407 CrossRef Medline
9. DeSouza, S., Fu, J., States, B. A., and Ziff, E. B. (2002) Differential palmitoylation directs the AMPA receptor-binding protein ABP to spines or to intracellular clusters. *J. Neurosci.* **22,** 3493–3503 CrossRef Medline
10. Brigidi, G. S., Sun, Y., Beccano-Kelly, D., Pitman, K., Mobasser, M., Borgland, S. L., Milnerwood, A. J., and Bamji, S. X. (2014) Palmitoylation of δ-catenin by DHHC5 mediates activity-induced synapse plasticity. *Nat. Neurosci.* **17,** 522–532 CrossRef Medline
11. Keith, D. J., Sanderson, J. L., Gibson, E. S., Woolfrey, K. M., Robertson, H. R., Olszewski, K., Kang, R., El-Husseini, A., and Dell'acqua, M. L. (2012) Palmitoylation of A-kinase anchoring protein 79/150 regulates dendritic endosomal targeting and synaptic plasticity mechanisms. *J. Neurosci.* **32,** 7119–7136 CrossRef Medline
12. Woolfrey, K. M., Sanderson, J. L., and Dell'Acqua, M. L. (2015) The palmitoyl acyltransferase DHHC2 regulates recycling endosome exocytosis and synaptic potentiation through palmitoylation of AKAP79/150. *J. Neurosci.* **35,** 442–456 CrossRef Medline
13. Brigidi, G. S., Santyr, B., Shimell, J., Jovellar, B., and Bamji, S. X. (2015) Activity-regulated trafficking of the palmitoyl-acyl transferase DHHC5. *Nat. Commun.* **6,** 8200 CrossRef Medline
14. Niethammer, P., Delling, M., Sytnyk, V., Dityatev, A., Fukami, K., and Schachner, M. (2002) Cosignaling of NCAM via lipid rafts and the FGF receptor is required for neuritogenesis. *J. Cell Biol.* **157,** 521–532 CrossRef Medline
15. Hérincs, Z., Corset, V., Cahuzac, N., Furne, C., Castellani, V., Hueber, A. O., and Mehlen, P. (2005) DCC association with lipid rafts is required

for netrin-1-mediated axon guidance. *J. Cell Sci.* **118,** 1687–1692 CrossRef Medline
16. Prescott, G. R., Gorleku, O. A., Greaves, J., and Chamberlain, L. H. (2009) Palmitoylation of the synaptic vesicle fusion machinery. *J. Neurochem.* **110,** 1135–1149 CrossRef Medline
17. Mukai, J., Tamura, M., Fénelon, K., Rosen, A. M., Spellman, T. J., Kang, R., MacDermott, A. B., Karayiorgou, M., Gordon, J. A., and Gogos, J. A. (2015) Molecular substrates of altered axonal growth and brain connectivity in a mouse model of schizophrenia. *Neuron* **86,** 680–695 CrossRef Medline
18. Holland, S. M., and Thomas, G. M. (2017) Roles of palmitoylation in axon growth, degeneration and regeneration. *J. Neurosci. Res.* **95,** 1528–1539 CrossRef Medline
19. Summers, D. W., Milbrandt, J., and DiAntonio, A. (2018) Palmitoylation enables MAPK-dependent proteostasis of axon survival factors. *Proc. Natl. Acad. Sci. U. S. A.* **115,** E8746–E8754 CrossRef Medline
20. Abe, N., and Cavalli, V. (2008) Nerve injury signaling. *Curr. Opin. Neurobiol.* **18,** 276–283 CrossRef Medline
21. Rishal, I., and Fainzilber, M. (2014) Axon-soma communication in neuronal injury. *Nat. Rev. Neurosci.* **15,** 32–42 CrossRef Medline
22. Mok, S. A., Lund, K., and Campenot, R. B. (2009) A retrograde apoptotic signal originating in NGF-deprived distal axons of rat sympathetic neurons in compartmented cultures. *Cell Res.* **19,** 546–560 CrossRef Medline
23. Harrington, A. W., and Ginty, D. D. (2013) Long-distance retrograde neurotrophic factor signalling in neurons. *Nat. Rev. Neurosci.* **14,** 177–187 CrossRef Medline
24. Ghosh, A. S., Wang, B., Pozniak, C. D., Chen, M., Watts, R. J., and Lewcock, J. W. (2011) DLK induces developmental neuronal degeneration via selective regulation of proapoptotic JNK activity. *J. Cell Biol.* **194,** 751–764 CrossRef Medline
25. Simon, D. J., Pitts, J., Hertz, N. T., Yang, J., Yamagishi, Y., Olsen, O., Mark, M. T., Molina, H., and Tessier-Lavigne, M. (2016) Axon degeneration gated by retrograde activation of somatic pro-apoptotic signaling. *Cell* **164,** 1031–1045 CrossRef Medline
26. Shin, J. E., Cho, Y., Beirowski, B., Milbrandt, J., Cavalli, V., and DiAntonio, A. (2012) Dual leucine zipper kinase is required for retrograde injury signaling and axonal regeneration. *Neuron* **74,** 1015–1022 CrossRef Medline
27. Mahar, M., and Cavalli, V. (2018) Intrinsic mechanisms of neuronal axon regeneration. *Nat. Rev. Neurosci.* **19,** 323–337 CrossRef Medline
28. Holland, S. M., Collura, K. M., Ketschek, A., Noma, K., Ferguson, T. A., Jin, Y., Gallo, G., and Thomas, G. M. (2016) Palmitoylation controls DLK localization, interactions and activity to ensure effective axonal injury signaling. *Proc. Natl. Acad. Sci. U. S. A.* **113,** 763–768 CrossRef Medline
29. Serwa, R. A., Abaitua, F., Krause, E., Tate, E. W., and O'Hare, P. (2015) Systems analysis of protein fatty acylation in herpes simplex virus-infected cells using chemical proteomics. *Chem. Biol.* **22,** 1008–1017 CrossRef Medline
30. Wei, X., Song, H., and Semenkovich, C. F. (2014) Insulin-regulated protein palmitoylation impacts endothelial cell function. *Arterioscler. Thromb. Vasc. Biol.* **34,** 346–354 CrossRef Medline
31. Chesarino, N. M., Hach, J. C., Chen, J. L., Zaro, B. W., Rajaram, M. V., Turner, J., Schlesinger, L. S., Pratt, M. R., Hang, H. C., and Yount, J. S. (2014) Chemoproteomics reveals Toll-like receptor fatty acylation. *BMC Biol.* **12,** 91 CrossRef Medline
32. Sobocińska, J., Roszczenko-Jasińska, P., Zare?ba-Kozioł, M., Hromada-Judycka, A., Matveichuk, O. V., Traczyk, G., èukasiuk, K., and Kwiatkowska, K. (2018) Lipopolysaccharide up-regulates palmitoylated enzymes of the phosphatidylinositol cycle: an insight from proteomic studies. *Mol. Cell. Proteomics* **17,** 233–254 CrossRef Medline
33. Yang, W., Di Vizio, D., Kirchner, M., Steen, H., and Freeman, M. R. (2010) Proteome scale characterization of human *S*-acylated proteins in lipid raft-enriched and non-raft membranes. *Mol. Cell. Proteomics* **9,** 54–70 CrossRef Medline
34. Bauer, S., Kerr, B. J., and Patterson, P. H. (2007) The neuropoietic cytokine family in development, plasticity, disease and injury. *Nat. Rev. Neurosci.* **8,** 221–232 CrossRef Medline
35. Quarta, S., Baeumer, B. E., Scherbakov, N., Andratsch, M., Rose-John, S., Dechant, G., Bandtlow, C. E., and Kress, M. (2014) Peripheral nerve regeneration and NGF-dependent neurite outgrowth of adult sensory neurons converge on STAT3 phosphorylation downstream of neuropoietic cytokine receptor gp130. *J. Neurosci.* **34,** 13222–13233 CrossRef Medline
36. Stahl, N., Boulton, T. G., Farruggella, T., Ip, N. Y., Davis, S., Witthuhn, B. A., Quelle, F. W., Silvennoinen, O., Barbieri, G., and Pellegrini, S. and (1994) Association and activation of Jak-Tyk kinases by CNTF-LIF-OSM-IL-6 β receptor components. *Science* **263,** 92–95 CrossRef Medline
37. Carbia-Nagashima, A., and Arzt, E. (2004) Intracellular proteins and mechanisms involved in the control of gp130/JAK/STAT cytokine signaling. *IUBMB Life* **56,** 83–88 CrossRef Medline
38. Lerch, J. K., Kuo, F., Motti, D., Morris, R., Bixby, J. L., and Lemmon, V. P. (2012) Isoform diversity and regulation in peripheral and central neurons revealed through RNA-Seq. *PLoS ONE* **7,** e30417 CrossRef Medline
39. Usoskin, D., Furlan, A., Islam, S., Abdo, H., Lönnerberg, P., Lou, D., Hjerling-Leffler, J., Haeggström, J., Kharchenko, O., Kharchenko, P. V., Linnarsson, S., and Ernfors, P. (2015) Unbiased classification of sensory neuron types by large-scale single-cell RNA sequencing. *Nat. Neurosci.* **18,** 145–153 CrossRef Medline
40. Zeisel, A., Hochgerner, H., Lönnerberg, P., Johnsson, A., Memic, F., van der Zwan, J., Haring, M., Braun, E., Borm, L. E., La Manno, G., Codeluppi, S., Furlan, A., Lee, K., Skene, N., Harris, K. D., *et al.* (2018) Molecular architecture of the mouse nervous system. *Cell* **174,** 999–1014 CrossRef Medline
41. Scheib, J., and Höke, A. (2013) Advances in peripheral nerve regeneration. *Nat. Rev. Neurol.* **9,** 668–676 CrossRef Medline
42. Simon, D. J., Weimer, R. M., McLaughlin, T., Kallop, D., Stanger, K., Yang, J., O'Leary, D. D., Hannoush, R. N., and Tessier-Lavigne, M. (2012) A caspase cascade regulating developmental axon degeneration. *J Neurosci* **32,** 17540–17553 CrossRef Medline
43. Niu, J., Sanders, S. S., Jeong, H. J., Holland, S. M., Sun, Y., Collura, K. M., Hernandez, L., Huang, H., Hayden, M. R., Smith, G. M., Hu, Y., Jin, Y., and Thomas, G. M. (2020) Coupled control of distal axon integrity and somal responses to axonal damage by the palmitoyl acyltransferase ZDHHC17. *bioRxiv* CrossRef CrossRef
44. Gorleku, O. A., Barns, A. M., Prescott, G. R., Greaves, J., and Chamberlain, L. H. (2011) Endoplasmic reticulum localization of DHHC palmitoyltransferases mediated by lysine-based sorting signals. *J. Biol. Chem.* **286,** 39573–39584 CrossRef Medline
45. Ernst, A. M., Syed, S. A., Zaki, O., Bottanelli, F., Zheng, H., Hacke, M., Xi, Z., Rivera-Molina, F., Graham, M., Rebane, A. A., Bjorkholm, P., Baddeley, D., Toomre, D., Pincet, F., and Rothman, J. E. (2018) *S*-Palmitoylation sorts membrane cargo for anterograde transport in the Golgi. *Dev. Cell* **47,** 479–493.e7 CrossRef Medline
46. Taylor, A. M., Blurton-Jones, M., Rhee, S. W., Cribbs, D. H., Cotman, C. W., and Jeon, N. L. (2005) A microfluidic culture platform for CNS axonal injury, regeneration and transport. *Nat. Methods* **2,** 599–605 CrossRef Medline
47. Hirota, H., Chen, J., Betz, U. A., Rajewsky, K., Gu, Y., Ross, J., Jr., Müller, W., and Chien, K. R. (1999) Loss of a gp130 cardiac muscle cell survival pathway is a critical event in the onset of heart failure during biomechanical stress. *Cell* **97,** 189–198 CrossRef Medline
48. Plum, W., Tschaharganeh, D. F., Kroy, D. C., Corsten, E., Erschfeld, S., Dierssen, U., Wasmuth, H., Trautwein, C., and Streetz, K. L. (2010) Lack of glycoprotein 130/signal transducer and activator of transcription 3-mediated signaling in hepatocytes enhances chronic liver injury and fibrosis progression in a model of sclerosing cholangitis. *Am. J. Pathol.* **176,** 2236–2246 CrossRef Medline
49. Kroy, D. C., Beraza, N., Tschaharganeh, D. F., Sander, L. E., Erschfeld, S., Giebeler, A., Liedtke, C., Wasmuth, H. E., Trautwein, C., and Streetz, K. L. (2010) Lack of interleukin-6/glycoprotein 130/signal transducers and activators of transcription-3 signaling in hepatocytes predisposes to liver steatosis and injury in mice. *Hepatology* **51,** 463–473 CrossRef Medline
50. Janoschek, R., Plum, L., Koch, L., Münzberg, H., Diano, S., Shanabrough, M., Müller, W., Horvath, T. L., and Brüning, J. C. (2006) gp130 signaling in proopiomelanocortin neurons mediates the acute anorectic response to centrally applied ciliary neurotrophic factor. *Proc. Natl. Acad. Sci. U. S. A.* **103,** 10707–10712 CrossRef Medline

51. Rodig, S. J., Meraz, M. A., White, J. M., Lampe, P. A., Riley, J. K., Arthur, C. D., King, K. L., Sheehan, K. C., Yin, L., Pennica, D., Johnson, E. M., Jr., and Schreiber, R. D. (1998) Disruption of the Jak1 gene demonstrates obligatory and nonredundant roles of the Jaks in cytokine-induced biologic responses. *Cell* **93,** 373–383 CrossRef Medline
52. Curtis, R., Adryan, K. M., Zhu, Y., Harkness, P. J., Lindsay, R. M., and DiStefano, P. S. (1993) Retrograde axonal transport of ciliary neurotrophic factor is increased by peripheral nerve injury. *Nature* **365,** 253–255 CrossRef Medline
53. Howie, J., Reilly, L., Fraser, N. J., Vlachaki Walker, J. M., Wypijewski, K. J., Ashford, M. L., Calaghan, S. C., McClafferty, H., Tian, L., Shipston, M. J., Boguslavskyi, A., Shattock, M. J., and Fuller, W. (2014) Substrate recognition by the cell surface palmitoyl transferase DHHC5. *Proc. Natl. Acad. Sci. U. S. A.* **111,** 17534–17539 CrossRef Medline
54. Ohno, Y., Kihara, A., Sano, T., and Igarashi, Y. (2006) Intracellular localization and tissue-specific distribution of human and yeast DHHC cysteine-rich domain-containing proteins. *Biochim. Biophys. Acta* **1761,** 474–483 CrossRef Medline
55. He, M., Abdi, K. M., and Bennett, V. (2014) Ankyrin-G palmitoylation and βII-spectrin binding to phosphoinositide lipids drive lateral membrane assembly. *J. Cell Biol.* **206,** 273–288 CrossRef Medline
56. Heinrich, P. C., Behrmann, I., Müller-Newen, G., Schaper, F., and Graeve, L. (1998) Interleukin-6-type cytokine signalling through the gp130/Jak/STAT pathway. *Biochem. J.* **334,** 297–314 CrossRef Medline
57. Wan, J., Roth, A. F., Bailey, A. O., and Davis, N. G. (2007) Palmitoylated proteins: purification and identification. *Nat. Protoc.* **2,** 1573–1584 CrossRef Medline
58. Jennings, B. C., Nadolski, M. J., Ling, Y., Baker, M. B., Harrison, M. L., Deschenes, R. J., and Linder, M. E. (2009) 2-Bromopalmitate and 2-(2-hydroxy-5-nitro-benzylidene)-benzo[b]thiophen-3-one inhibit DHHC-mediated palmitoylation *in vitro*. *J. Lipid Res.* **50,** 233–242 CrossRef Medline
59. Kilpatrick, C. L., Murakami, S., Feng, M., Wu, X., Lal, R., Chen, G., Du, K., and Luscher, B. (2016) Dissociation of Golgi-associated DHHC-type zinc finger protein (GODZ)- and Sertoli cell gene with a zinc finger domain-β (SERZ-β)-mediated palmitoylation by loss of function analyses in knockout mice. *J. Biol. Chem.* **291,** 27371–27386 CrossRef Medline
60. Raymond, F. L., Tarpey, P. S., Edkins, S., Tofts, C., O'Meara, S., Teague, J., Butler, A., Stevens, C., Barthorpe, S., Buck, G., Cole, J., Dicks, E., Gray, K., Halliday, K., Hills, K., *et al.* (2007) Mutations in ZDHHC9, which encodes a palmitoyltransferase of NRAS and HRAS, cause X-linked mental retardation associated with a Marfanoid habitus. *Am. J. Hum. Genet.* **80,** 982–987 CrossRef Medline
61. Mansouri, M. R., Marklund, L., Gustavsson, P., Davey, E., Carlsson, B., Larsson, C., White, I., Gustavson, K. H., and Dahl, N. (2005) Loss of ZDHHC15 expression in a woman with a balanced translocation t(X;15)(q13.3;cen) and severe mental retardation. *Eur. J. Hum. Genet.* **13,** 970–977 CrossRef Medline
62. Sanders, S. S., Parsons, M. P., Mui, K. K., Southwell, A. L., Franciosi, S., Cheung, D., Waltl, S., Raymond, L. A., and Hayden, M. R. (2016) Sudden death due to paralysis and synaptic and behavioral deficits when Hip14/Zdhhc17 is deleted in adult mice. *BMC Biol.* **14,** 108 CrossRef Medline
63. Mukai, J., Liu, H., Burt, R. A., Swor, D. E., Lai, W. S., Karayiorgou, M., and Gogos, J. A. (2004) Evidence that the gene encoding ZDHHC8 contributes to the risk of schizophrenia. *Nat. Genet.* **36,** 725–731 CrossRef Medline
64. Noritake, J., Fukata, Y., Iwanaga, T., Hosomi, N., Tsutsumi, R., Matsuda, N., Tani, H., Iwanari, H., Mochizuki, Y., Kodama, T., Matsuura, Y., Bredt, D. S., Hamakubo, T., and Fukata, M. (2009) Mobile DHHC palmitoylating enzyme mediates activity-sensitive synaptic targeting of PSD-95. *J. Cell Biol.* **186,** 147–160 CrossRef Medline
65. Oku, S., Takahashi, N., Fukata, Y., and Fukata, M. (2013) *In silico* screening for palmitoyl substrates reveals a role for DHHC1/3/10 (zDHHC1/3/11)-mediated neurochondrin palmitoylation in its targeting to Rab5-positive endosomes. *J. Biol. Chem.* **288,** 19816–19829 CrossRef Medline
66. Chen, M. L., Cheng, C., Lv, Q. S., Guo, Z. Q., Gao, Y., Gao, S. F., Li, X., Niu, S. Q., Shi, S. X., and Shen, A. G. (2008) Altered gene expression of NIDD in dorsal root ganglia and spinal cord of rats with neuropathic or inflammatory pain. *J. Mol. Histol.* **39,** 125–133 CrossRef Medline
67. Li, Y., Martin, B. R., Cravatt, B. F., and Hofmann, S. L. (2012) DHHC5 protein palmitoylates flotillin-2 and is rapidly degraded on induction of neuronal differentiation in cultured cells. *J. Biol. Chem.* **287,** 523–530 CrossRef Medline
68. Lorent, J. H., and Levental, I. (2015) Structural determinants of protein partitioning into ordered membrane domains and lipid rafts. *Chem. Phys. Lipids* **192,** 23–32 CrossRef Medline
69. Houck, K. L., Yuan, H., Tian, Y., Solomon, M., Cramer, D., Liu, K., Zhou, Z., Wu, X., Zhang, J., Oehler, V., and Dong, J. F. (2019) Physical proximity and functional cooperation of glycoprotein 130 and glycoprotein VI in platelet membrane lipid rafts. *J. Thromb. Haemost.* **17,** 1500–1510 CrossRef Medline
70. Allen, M. J., Fan, Y. Y., Monk, J. M., Hou, T. Y., Barhoumi, R., McMurray, D. N., and Chapkin, R. S. (2014) *n*-3 PUFAs reduce T-helper 17 cell differentiation by decreasing responsiveness to interleukin-6 in isolated mouse splenic $CD4^+$ T cells. *J. Nutr.* **144,** 1306–1313 CrossRef Medline
71. Port, M. D., Gibson, R. M., and Nathanson, N. M. (2007) Differential stimulation-induced receptor localization in lipid rafts for interleukin-6 family cytokines signaling through the gp130/leukemia inhibitory factor receptor complex. *J. Neurochem.* **101,** 782–793 CrossRef Medline
72. Lee, M. Y., Ryu, J. M., Lee, S. H., Park, J. H., and Han, H. J. (2010) Lipid rafts play an important role for maintenance of embryonic stem cell self-renewal. *J. Lipid Res.* **51,** 2082–2089 CrossRef Medline
73. Yanagisawa, M., Nakamura, K., and Taga, T. (2004) Roles of lipid rafts in integrin-dependent adhesion and gp130 signalling pathway in mouse embryonic neural precursor cells. *Genes Cells* **9,** 801–809 CrossRef Medline
74. Buk, D. M., Waibel, M., Braig, C., Martens, A. S., Heinrich, P. C., and Graeve, L. (2004) Polarity and lipid raft association of the components of the ciliary neurotrophic factor receptor complex in Madin-Darby canine kidney cells. *J. Cell Sci.* **117,** 2063–2075 CrossRef Medline
75. Davis, S., Aldrich, T. H., Valenzuela, D. M., Wong, V. V., Furth, M. E., Squinto, S. P., and Yancopoulos, G. D. (1991) The receptor for ciliary neurotrophic factor. *Science* **253,** 59–63 CrossRef Medline
76. Blanc, M., David, F., Abrami, L., Migliozzi, D., Armand, F., Bürgi, J., and van der Goot, F. G. (2015) SwissPalm: protein palmitoylation database. *F1000Res* **4,** 261 CrossRef Medline
77. Milde, S., Gilley, J., and Coleman, M. P. (2013) Subcellular localization determines the stability and axon protective capacity of axon survival factor Nmnat2. *PLoS Biol.* **11,** e1001539 CrossRef Medline
78. Maday, S., Wallace, K. E., and Holzbaur, E. L. (2012) Autophagosomes initiate distally and mature during transport toward the cell soma in primary neurons. *J. Cell Biol.* **196,** 407–417 CrossRef Medline
79. Maday, S., Twelvetrees, A. E., Moughamian, A. J., and Holzbaur, E. L. (2014) Axonal transport: cargo-specific mechanisms of motility and regulation. *Neuron* **84,** 292–309 CrossRef Medline
80. Guedes-Dias, P., and Holzbaur, E. L. F. (2019) Axonal transport: driving synaptic function. *Science* **366,** eaaw9997 CrossRef Medline
81. Sleigh, J. N., Rossor, A. M., Fellows, A. D., Tosolini, A. P., and Schiavo, G. (2019) Axonal transport and neurological disease. *Nat. Rev. Neurol.* **15,** 691–703 CrossRef Medline
82. Park, J. W., Vahidi, B., Taylor, A. M., Rhee, S. W., and Jeon, N. L. (2006) Microfluidic culture platform for neuroscience research. *Nat. Protoc.* **1,** 2128–2136 CrossRef Medline